DOI: 10.1002/adma.200700225

Nanoimprint Lithography Based Approach for the Fabrication of Large-Area, Uniformly Oriented Plasmonic Arrays**

By *Brandon D. Lucas, Jin-Sung Kim, Christine Chin,* and *L. Jay Guo**

Localized surface plasmon resonance (LSPR), collective electron density oscillations found in noble metal nanostructures, has been studied extensively over the past decade due to its potential utility as the backbone for a number of photonic technologies capable of controlling light at nanoscopic dimensions well below the diffraction limit.[1,2] Research in this field has been engendered by the tremendous growth in fabrication methods capable of producing an enormous variety of nanoparticle (NP) systems and nanostructured films. Numerous theoretical and experimental studies have established that LSPR is sensitive to the shape, size, interparticle distance, dielectric environment and material composition of the constituent NPs.[3–6] Additionally, optical dichroism observed from well-aligned nanoparticle arrays has demonstrated the polarization dependence of their LSPR response.[7–9] One of the most promising applications of nanoparticle systems is their use as real-time chemical and biological sensors that originate from the aforementioned LSPR dependence on their dielectric environment. Such systems have been demonstrated using a variety of NP implementations including single-particle, one-dimensional and two-dimensional array configurations on transparent substrates as well as solution-based methods.[10,11]

An abundance of nanofabrication techniques have been employed to produce the desired nanostructures utilized in LSPR studies with varied degrees of success as measured by parameters such as monodispersity. A few examples of these techniques include electron beam lithography, templates, nanosphere lithography (NSL) and colloidal solution-based nanoparticle synthesis—of which the latter two have been used quite extensively.[4,12–14] Although NSL and solution-based methods have been effective for fundamental studies of the influence of NP characteristics on LSPR, there are still significant limitations of both techniques that limit their applicability to commercialized LSPR-based applications.

Chemical synthesis techniques have the advantage of creating a wide array of exotic nanostructures based on modification of the reaction parameters such as time, relative concentration of reactants and temperature. However, the monodispersity and reproducibility of desired structures can be difficult to achieve using this method. More importantly, this technique lacks the control of relative NP positioning and orientation in addition to the requirement of novel surface chemistries for the reduction of NP agglomeration and effective substrate attachment. The inability to precisely control the sample-to-sample LSPR response of immobilized NP systems is a severe limitation of this fabrication approach.

Nanosphere lithography is an alternative fabrication method introduced by Hulteen et al. to produce periodic particle arrays (PPAs) directly on a variety of substrates. This technique utilizes a closed-packed nanosphere mask that permits direct deposition of noble metal NPs onto a substrate through the interstitial regions of the mask. NSL has been implemented in a single-layer and double-layer approach with extensive characterization and utilization of triangular nanoparticles resulting from the single-layer method. The precise control of PPA attributes afforded by this technique makes it a promising candidate as a fabrication method relevant to commercialized LSPR applications. Limitations of NSL include issues with surface coverage and the geometric constraints imposed by the nanosphere mask on the PPA lattice structure and NP shape characteristics which reduce the degrees-of-freedom available for the designed LSPR response of the PPA system.

In order to address and supplement limitations encountered by a number of current NP fabrication methods, we propose the use of Nanoimprint Lithography (NIL) and two-dimensional nanostructure array (*nanoblock*) molds derived from one-dimensional gratings to produce noble metal NPAs. We believe this approach possesses a number of attributes that will not only enhance the fundamental study of NP systems, but may also play a key role in the production of marketable LSPR technologies. First, NIL is a mold-based, high-throughput and low-cost process capable of patterning large areas with sub-10 nm

[*] Prof. L. J. Guo, Dr. J.-S. Kim
Department of Electrical Engineering and Computer Science,
University of Michigan Solid State Electronics Laboratory,
1301 Beal Ave., Ann Arbor, MI 48109
E-mail: guo@umich.edu

B. D. Lucas
University of Michigan-Applied Physics
2477 Randall Laboratory
450 Church St., Ann Arbor, MI48109 (USA)

C. Chin
Massachusetts Institute of Technology,
Department of Mechanical Engineering,
77 Massachusetts Ave., Cambridge, MA 02139

[**] B. D. L. and J.-S. K. contributed equally to this work. This work is supported by CDC grant with a subcontract from Duke University No. 04-SC-CDC-1012, an AFOSR grant FA9550-06-1-0510, an NSFC grant no. 60528003, and a NATO grant CBP.NUKR.CLG 981776. B. Lucas would like to thank the David and Lucile Packard Foundation and UNCF-Merck Science Initiative for their generous support.

 © 2008 WILEY-VCH Verlag GmbH & Co. KGaA,Weinheim

ADVANCED MATERIALS

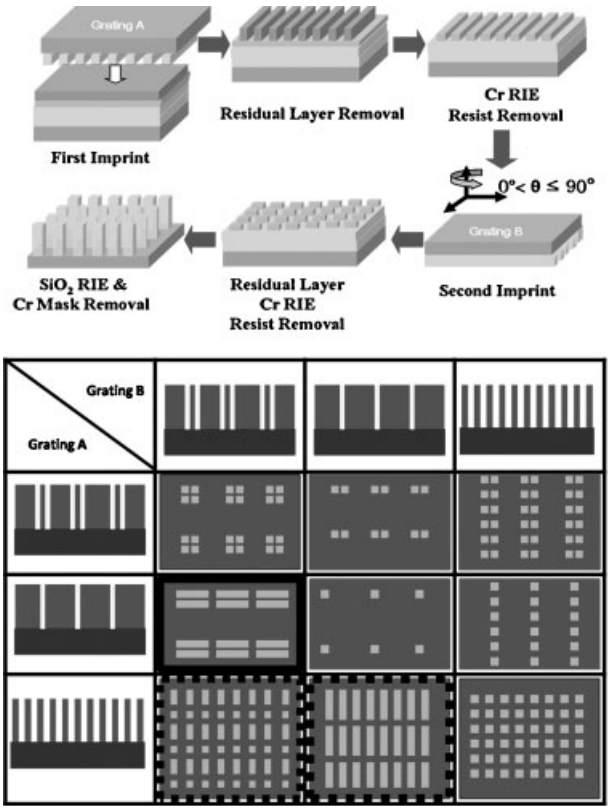

Figure 1. (Top) Illustration of the general process used to fabricate ''nanoblock'' molds possessing different lattice and particle geometries. (Bottom) Matrix illustrating possible nanoparticle array configurations from A90B nanoblock molds produced using a collection of one-dimensional grating molds with different profiles. The array bordered by a solid line is produced using the inverse profile of grating A. Similarly, the arrays bordered by broken lines are achieved using the inverse of grating B.

resolution.[15,16] Second, the benefits of alternative nanofabrication methods capable of creating unique LSPR nanostructures and possessing less desirable throughput and cost characteristics can be maximized through their use for creation of NIL molds that enable the perpetual reproduction of these structures. This characteristic of NIL to ''preserve'' nanostructures in a mold permits the optimization of NPAs for particular LSPR applications through empiricism. Moreover, the use of one-dimensional grating structures as the foundation to create NPAs enables resulting two-dimensional patterns of varying complexity to be geometrically interpreted and modeled for design purposes.

In this communication, we explore a NIL fabrication approach capable of creating uniformly oriented and homogenous noble metal NPAs. Extensions of this fabrication method demonstrating the flexibility of this technique to produce NPAs possessing a variety of unique structural and LSPR characteristics are demonstrated. The relevance of this method is further elucidated by exploring the consequences of these interesting findings within the context of previous works. We believe this to be the first report of such a NIL-based fabrication approach for the production of plasmonic NPAs.

Illustrated in Figure 1 is the general approach used to create large-area molds that are subsequently used to fabricate NPAs. First, a suitable substrate is coated with a mask layer and spincoated with nanoimprint resist. The resist is patterned using a one-dimensional grating mold (A) and the pattern is transferred to the underlying mask layer (e.g. Cr) through a suitable etching process. After removing the previously patterned resist, a new layer of resist is applied for a second imprint with a one-dimensional grating mold (B) rotated θ relative to the previous imprint. The pattern is again transferred to the underlying mask layer by an etch process resulting in a two-dimensionally patterned mask layer that is subsequently used to produce a two-dimensional array of ''nanoblocks'' in the substrate material through a suitable anisotropic etch process. Large-area metallic NPAs are produced by these nanoblock molds through conventional NIL processing steps consisting of imprinting, residual polymer removal, metallization and lift-off.

This technique is extremely powerful in creating a variety of structures by simply using one-dimensional gratings with differences in their lateral characteristics (i.e. duty cycle or period) and relative angular orientation θ for successive imprints. Benefiting this technique are the numerous realized methods used to produce, modify and optimize one-dimensional grating structures.[17–20] For example, if the same grating mold is used and oriented orthogonally for successive imprints (A90A), a square lattice of rectangular or cylindrical (due to the reduced anisotropy of the etching process) nanoblocks (Figs. 2B and C) are realized. However, if this same process is repeated with a non-orthogonal orientation for successive imprints such as $\theta = 45°$, an array of diamond nanoblocks is produced on a rhomboidal lattice (Fig. 2A). Likewise, if two different grating structures are utilized in a AθB scheme, it is possible to create two-dimensional lattices of rectangular ($\theta = 90$, Fig. 2D) and diamond nanoblocks ($90 > \theta > 0$). Consequently three unique NPAs (AθA, AθB, BθB) are possible by simply using a combination of two different grating structures at one particular relative orientation θ.

NPAs with interparticle distances that allow them to behave effectively as single NPs or highly coupled NP systems are

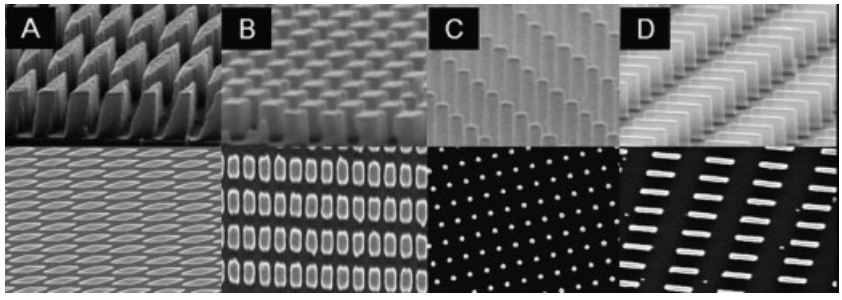

Figure 2. SEMs of representative nanoblock molds derived from one-dimensional gratings using (A) A45A, (B-C) A90A and (D) A90B schemes.

 © 2008 WILEY-VCH Verlag GmbH & Co. KGaA,Weinheim

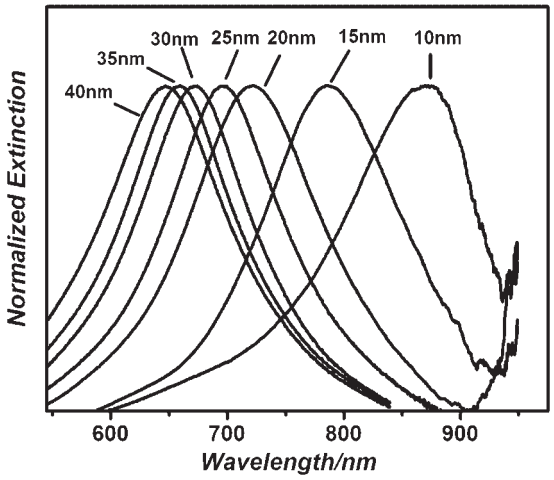

Figure 3. Au square NPA (1nm Ti adhesion layer) with varying nanostructure height demonstrating the inverse relationship between NP height and LSPR peak wavelength.

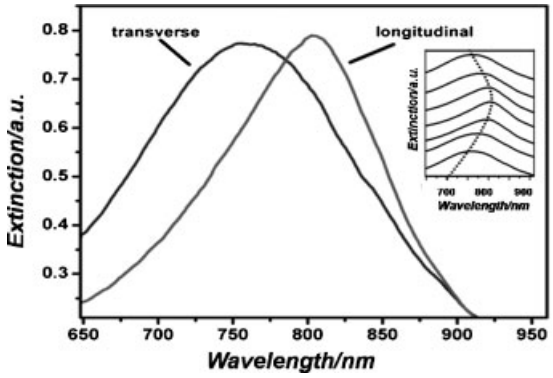

Figure 4. Extinction spectra corresponding to light polarized along the short axis (transverse mode) and long axis (longitudinal mode) of the NPA. (Inset) Offset extinction spectrum of Au NPA (height = 3 nmTi/20 nm Au; length = 128 nm; width = 115 nm) embedded in 300 nm film of 950 K PMMA with 30° difference in polarizer position for successive spectra. The peak position is tracked by a dotted line for clarity.

possible by combining gratings with the appropriate line density. For example, a large area of one-dimensional NP chains in different structural formats (e.g. single particle, dimers, etc.) are feasible using low and high line density gratings in an A90B scheme with single period or multi-period one-dimensional gratings. Similar structures have demonstrated narrow plasmon peaks and excellent potential LSPR sensing capabilities.[21] Likewise, effectively isolated NPs are possible by combining two low-density gratings. Additionally, more complex NPAs are achievable by creating composite molds that combine multiple two-dimensional nanoblock molds.

The flexibility and utility of this fabrication approach is further highlighted by the numerous studies resulting from nanostructures derivable by this technique. A great deal of interest in nanostructured thin films currently exists due to their surface plasmon- enhanced transmission properties and potential applications.[22] These nanopatterned films are accessible using this technique by simply creating the negative of the nanoblock molds and employing conventional NIL or using a recently demonstrated negative-tone NIL process (n-NIL).[23] NSL produced nanowell structures have been demonstrated by Hicks et. al. to produce narrow LSPR peaks and enhanced sensitivity to dielectric changes.[24] These structures are achievable using our NIL-based technique by imprinting with a NPA mold of the proper depth and using the appropriate metallization. The use of NIL inherently increases throughput and reduces the cost associated with producing such a structure in addition to simplifying the fabrication through the elimination of RIE. As over ten billion nanoparticles are created using a nanoblock mold derived from 200 nm period gratings covering an area of 1 cm^2, NPs can be massively produced, functionalized and released from their substrate for use in a solution-phase detection scheme.[25]

An ideal method to produce LSPR nanostructures would permit the optimization of their response for a specific application such as surface enhanced Raman spectroscopy (SERS) where it has been previously shown that the electromagnetic enhancement of specific Raman bands are influenced by their relative position to the LSPR of the substrate. This tunability aspect is demonstrated in Figure 3 for Au NPAs only differing in their nanostructure height. A blue shift in the LSPR of the NPAs for both Au and Ag was found to occur for increasing height of the nanostructures. Readily apparent from this data is the nonlinearity of wavelength shift as a function of nanoparticle height. We believe that this can be attributed to the influence of the increasing proximity of the LSPR to a wavelength region

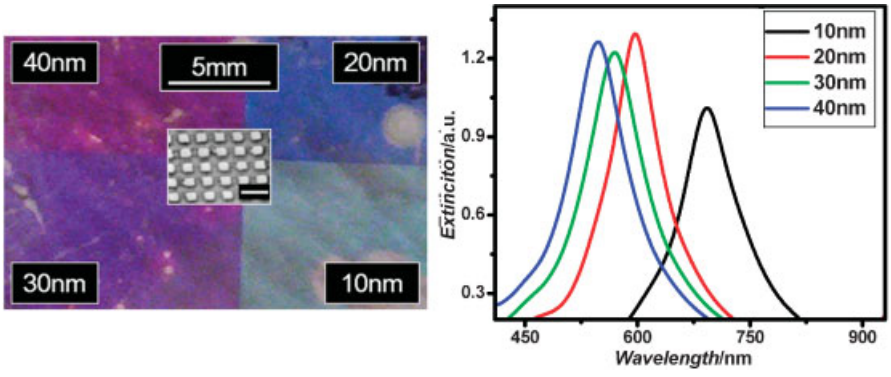

Figure 5. (*Left*) Photograph of a Ag sample possessing four distinct areas of structures that differ in metal thickness as indicated by the labels. SEM micrograph of the NPA is shown as an inset (scale bar = 350 nm). (*Right*) Measured extinction spectra corresponding to the four distinct areas shown in the photograph.

© 2008 WILEY-VCH Verlag GmbH & Co. KGaA,Weinheim

ADVANCED MATERIALS

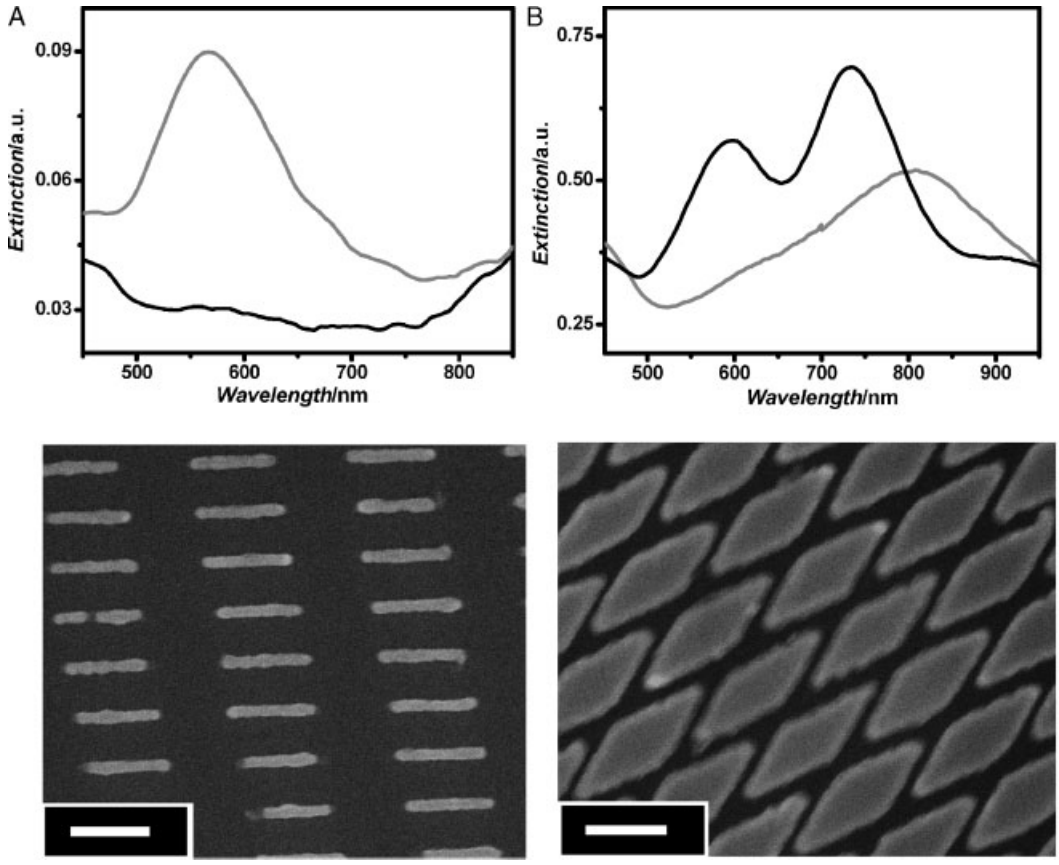

Figure 6. (A) Extinction spectra obtained on Au nanorod array for orthogonal linear polarizations. Due to the high degree of anisotropy possessed by the constituent NPs, the resonances are spectrally isolated. (B) By creating a densely-packed A45B Au nanodiamond array, two resonances are excited by one linear polarizaton state. The orthogonal polarizatoin completely extinguishes the aforementioned response and yields a broad extinction peak. SEM micrographs shown below the corresponding extinction spectra; scale bars =350 nm.

where additional material dependent resonances characteristic of Au (e.g. interband transitions) occur (Fig. 4).

Various methods have demonstrated the ability to align rod-like nanostructures by incorporating them into a polymer matrix to create nanocomposite films possessing polarization dependent optical properties. Dirix et al. used stretching of a polymer-NP nanocomposite film to create a ''pearl-necklace'' alignment of the constituent Ag NPs.[7] As a result of this induced alignment, the nanocomposite film achieved very distinct colors when viewed using linearly polarized light. For the square nanoblocks shown in the insert of Figure 5, although the in-plane aspect ratio of the structures are approximately unity, there is still a clear distinction between the LSPR response of normally incident light polarized along the short-axis and the long-axis. For light linearly polarized along the short axis the resonance occurs at the highest energy (transverse). Conversely, light polarized along the long axis of the structure yields a resonance at the lowest energy (longitudinal). The ability to distinguish the two modes with a collection of nanostructures possessing a diminutive shape anisotropy is a direct result of the orientational control afforded by the NIL fabrication technique as opposed to the ensemble average response of chemically synthesized nanostructures. This shape anisotropy can be attributed to slight differences in etching characteristics during mold fabrication using orthogonal imprints with the same one-dimensional grating mold.

Changing the material composition of the constituent nanostructures from Au to Ag yields a resonance that occurs more towards the center of the visible spectrum (Fig. 5). As a result of this material dependence, the difference in optical properties for nanostructures differing in height by 10nm is clearly observed through their pronounced difference in color. Similar to the case for Au, the resonance is more blue-shifted for the taller nanostructures. It is also interesting to note the significant increase in extinction occurring between the 10 nm and 20 nm dimensions which suggest that increased damping due to surface scattering may play a non-negligible role. Additionally, the strength of our large-area fabrication approach is manifested through the ability to fabricate four distinct areas possessing different resonances on one substrate.

Using this basic technique, arrays possessing nanostructures with greater anisotropy can yield plasmonic responses with very different characteristics. As shown in Figure 6(A), by using two molds possessing different periods orthogonally (A90B), it is

 © 2008 WILEY-VCH Verlag GmbH & Co. KGaA,Weinheim

possible to produce arrayed nanorod structures with a well-resolved transverse mode as opposed to the nearly degenerate modes of the square nanoblock array. As shown in Figure 5, the resulting extinction spectrum from the nanorods shows a transverse mode resonance peak at 560 nm that can be totally extinguished by using an orthogonal linear polarization state. The expected longitudinal response appears to occur at wavelengths out of the spectral range of the spectrometer used in our experiment.

Another exemplary result demonstrating the potential of this fabrication approach is found for an A45A array. This combination yields an array with a diamond motif that possesses unique polarization sensitive plasmonic responses. The most contrasting results for two orthogonal polarizations are shown in Figure 6(B). For the same polarization there exist two distinguishable peak features around 580 nm and 720 nm. While the other polarization yields one broad resonance around 805 nm. This rich, polarization-dependent response of these ''nanodiamonds'' may be attributable to their increased size parameters which considerably exceed the dipolar approximation. As the dimensions of these structures and the interparticle distances are both on the order of the resonant wavelengths of the broadband light source, we believe that a unique combination of near-field coupling, diffractive far-field coupling and retardation effects play prominently in these intriguing experimental results.

To fully highlight the potential of this fabrication approach, we will briefly discuss applications of these NIL derived NPAs that are the focus of our current research efforts. The ability of nanoparticles to behave as label-free biosensors has been propelled by numerous advances in surface chemistry permitting the detection of numerous biological interactions. It is plausible that using NIL as the method to fabricate NPAs will open the possibility to play a significant role in medical science research and point-of-care diagnostics. Many previous works have centered on using the robust signal of peak wavelength shift to monitor these changes, however, the resulting change in extinction intensity at a single wavelength is more difficult to utilize due to reasons including signal-to-noise limitations. Through the creation of plasmonic microtiter plates using NIL as the low-cost production method, we believe it will be possible to utilize conventional single wavelength microplate-readers for multiparallel assays. Such a device would permit extremely low sample consumption since detection only requires dielectric changes due to biological interactions within the nanoenvironment of the constituent NPs. Secondly, the detection wavelength for the system is selected based on the resonance wavelength of the NPA which exists well away from UV wavelengths that may lead to photodegradation of biological samples. Thirdly, as the nominal transmission of these arrays is >50%, it is possible to create double-sided chips that utilize the polarization selectivity of anisotropic NPs. For instance, nanorods on opposite sides of the substrate could be oriented orthogonally with respect to each other and subsequently interrogated for their individual response by using the appropriate linear polarization state. Furthermore, the resonance control and transparency of these chips permit their vertical assembly into a plasmonic sensor stack.

Recent work by Zhao et al.[27] has also provided the opportunity for this technique to better exploit findings related to the interaction of plasmonic and molecular resonances. Previous work has used NSL derived arrays with the requisite variation of plasmonic resonances achieved through the NP material thickness dependence. A technique that permits in-situ selection of the resonance wavelength greatly benefits applications based on this phenomenon by reducing sample consumption and transport requirements. The polarization sensitive near-unity aspect ratio NPAs produced by NIL are an ideal candidate to optimize the utilization of this effect to produce fine-tuned LSPR response. By simply changing the input linear polarization state in a controlled manner, it is possible to achieve a continuum of resonances within an approximately 50 nm bandwidth.

Lastly, there is tremendous interest in using metallic NPAs as enhancing substrates for Raman and fluorescence techniques. Specifically, detailed work elucidating the dominant electromagnetic enhancement effect has shown that the Raman signal of the absorbate is maximally enhanced when the plasmonic response is energetically positioned near the midpoint between the excitation source and Raman band.[26] It is believed that this situation permits the optimal plasmonic enhancement of both incident and Raman-shifted radiation. By utilizing SERS substrates similar to the nanodiamond array that supports multiple plasmons, a broader range of absorbate Raman bands can be enhanced.

In summary, we presented a very powerful and flexible approach to fabricate large-area, uniformly-oriented noble metal NPAs using NIL and one-dimensional gratings that we believe will have tremendous impact on a number of LSPR applications including tunable filters, LSPR-based sensors and surface-enhanced spectroscopies. We demonstrated the flexibility of this approach by complete control of the plasmonic response of NPAs through their composition, size and shape. Moreover, the inherent orientational control of this fabrication technique was demonstrated through the acquisition of remarkable polarization dependent extinction spectra. We believe this is a commercially relevant NPA production method that will enhance previously realized applications, such as LSPR biosensor chips, and facilitate the expansion into newer domains which is the focus of our current research efforts.

Experimental

Nanoblock Mold Fabrication: Nanoblock mold used in this study was fabricated using the A90A scheme. A thin 10 nm film of Cr serving as the mask layer was electron beam evaporated on 200 nm thermally grown SiO_2. The nanoimprint resist (*MicroResist MR- i-8020;* $T_g = 115\,^{\circ}C$) was spincoated on the substrate to the appropriate thickness (determined by mold depth, duty cycle and period), baked on hotplate (140 °C; 5 min) to remove residual solvent and imprinted in a custom-built nanoimprinter (670 psi; 5 min.; 180 °C). After separation of the mold and substrate, the

© 2008 WILEY-VCH Verlag GmbH & Co. KGaA,Weinheim

ADVANCED MATERIALS

residual polymer was removed in an O^2 plasma and the pattern was transferred to the Cr layer using RIE (40/8 sccm Cl_2/O_2; 200 W; 150 mT). The resist was stripped using an Acetone soak, rinsed with Methanol and IPA and dried using N_2. The above process steps were repeated for the second imprint and the 200 nm SiO_2 was subsequently reactive-ion etched (20 sccm CHF_3; 20 mT; 150 W) using the patterned Cr mask. After etching, the Cr mask was removed using a wet chromium etchant (*CR-14; Cyantek Co.*), rinsed with a copious amount of deionized water (DI:H_2O) and dried with N_2. The mold was then prepared for imprinting by vapor-phase surfactant treatment to reduce mold-polymer adhesion.

Sample Fabrication: Pyrex glass substrates were cleaned in a 1:1 pirhanna solution (30% H_2O_2: 29%NH_4OH), rinsed with a copious amount of DI:H_2O and dried using N_2. The resist was spincoated to the appropriate thickness on the substrate, baked on a hotplate for solvent removal and imprinted. After separation, the residual polymer layer was removed using O_2 plasma reactive-ion etching. Metallization was accomplished using an electron beam evaporator by first depositing a 1-3 nm Ti adhesion layer followed by the mass thickness of Au or Ag as determined by the in-situ monitoring system. Lift-off was performed by soaking the sample in Acetone and using a low-power ultrasonic bath. After completion of lift-off, samples w ere rinsed with methanol and IPA and dried with N_2.

Extinction Measurements: All extinction measurements were acquired using a Nikon TE300 Eclipse inverted microscope (20× objective; NA = 0.44) with transmitted light coupled into an Ocean Optics fiber-coupled spectrometer (HR-4000 or SD-2000) using an achromatic lens. For polarization dependent extinction measurements, a linear polarizer mounted in a rotating module was aligned to the optic-axis of the microscope directly above the sample stage. All measurements were taken using normally incident light and referenced to unpatterned glass.

Received: January 26, 2007
Revised: October 1, 2007

[1] S. A. Maier, *Curr. Nanosci.* **2005**, *1*, 17.
[2] H. A. Atwater, S. Maier, A. Polman, J. A. Dionne, L. Sweatlock, *MRS Bull.* **2005**, *30*, 385.
[3] J. J. Mock, D. R. Smith, S. Schultz, *Nano Lett.* **2003**, *3*, 485.
[4] J. J. Mock, M. Barbic, D. R. Smith, D. A. Schultz, S. Schultz, *J. Chem. Phys.* **2002**, *116*, 6755.
[5] K. H. Su, Q. H. Wei, X. Zhang, J. J. Mock, D. R. Smith, S. Schultz, *Nano Lett.* **2003**, *3*, 1087.
[6] M. D. Malinsky, K. L. Kelly, G. C. Schatz, R. P. Van Duyne, *J. Phys. Chem. B* **2001**, *105*, 2343.
[7] Y. Dirix, C. Bastiaansen, W. Caseri, P. Smith, *Adv. Mater.* **1999**, *11*, 223.
[8] C. L. Haynes, R. P. Van Duyne, *Nano Lett.* **2003**, *3*, 939.
[9] B. K. Canfield, S. Kujala, M. Kauranen, K. Jefimovs, T. Vallius, J. Turunen, *Appl. Phys. Lett.* **2005**, 86.
[10] A. D. McFarland, R. P. Van Duyne, *Nano Lett.* **2003**, *3*, 1057.
[11] N. Nath, A. Chilkoti, *Analyt. Chem.* **2002**, *74*, 504.
[12] S. J. Oldenburg, G. D. Hale, J. B. Jackson, N. J. Halas, *Appl. Phys. Lett.* **1999**, *75*, 1063.
[13] L. J. Sherry, S. H. Chang, G. C. Schatz, R. P. Van Duyne, B. J. Wiley, Y. N. Xia, *Nano Lett.* **2005**, *5*, 2034.
[14] A. Bouhelier, R. Bachelot, J. S. Im, G. P. Wiederrecht, G. Lerondel, S. Kostcheev, P. Royer, *J. Phys. Chem. B* **2005**, *109*, 3195.
[15] S. Y. Chou, P. R. Krauss, *Microelectron. Eng.* **1997**, *35*, 237.
[16] M. T. Li, L. Chen, W. Zhang, S. Y. Chou, *Nanotechnology* **2003**, *14*, 33.
[17] Z. N. Yu, S. Y. Chou, *Nano Lett.* **2004**, *4*, 341.
[18] Z. N. Yu, W. Wu, L. Chen, S. Y. Chou, *J. Vac. Sci. Technol. B* **2001**, *19*, 2816.
[19] Z. N. Yu, L. Chen, W. Wu, H. X. Ge, S. Y. Chou, *J. Vac. Sci. Technol. B* **2003**, *21*, 2089.
[20] X. Y. Lei, L. Wu, P. Deshpande, Z. N. Yu, W. Wu, H. X. Ge, S. Y. Chou, *Nanotechnology* **2003**, *14*, 786.
[21] E. M. Hicks, S. L. Zou, G. C. Schatz, K. G. Spears, R. P. Van Duyne, L. Gunnarsson, T. Rindzevicius, B. Kasemo, M. Kall, *Nano Lett.* **2005**, *5*, 1065.
[22] T. W. Ebbesen, H. J. Lezec, H. F. Ghaemi, T. Thio, P. A. Wolff, *Nature* **1998**, *391*, 667.
[23] L. Y. Jiao, H. J. Gao, G. M. Zhang, G. Y. Xie, X. Zhou, Y. Y. Zhang, Y. Y. Zhang, B. Gao, G. Luo, Z. Y. Wu, T. Zhu, J. Zhang, Z. F. Liu, S. C. Mu, H. F. Yang, C. Z. Gu, *Nanotechnology* **2005**, *16*, 2779.
[24] E. M. Hicks, X. Y. Zhang, S. L. Zou, O. Lyandres, K. G. Spears, G. C. Schatz, R. P. Van Duyne, *J. Phys. Chem. B* **2005**, *109*, 22351.
[25] A. J. Haes, J. Zhao, S. L. Zou, C. S. Own, L. D. Marks, G. C. Schatz, R. P. Van Duyne, *J. Physical Chem. B* **2005**, *109*, 11158.
[26] A. D. McFarland, M. A. Young, J. A. Dieringer, R. P. Van Duyne, *J. Phys. Chem. B* **2005**, *109*, 11279.
[27] J. Zhao, L. Jensen, J. H. Sung, S. L. Zou, G. C. Schatz, R. P. Van Duyne, *J. Am. Chem. Soc.* **2007**, *129*, 7647.

 © 2008 WILEY-VCH Verlag GmbH & Co. KGaA,Weinheim